NEURAL REGENERATION RESEARCH
www.nrronline.org

Research Article

# Biochanin A attenuates spinal cord injury in rats during early stages by inhibiting oxidative stress and inflammasome activation

Xigong Li[1, #], Jing Fu[2, #], Ming Guan[1], Haifei Shi[1], Wenming Pan[3, *], Xianfeng Lou[1, *]

https://doi.org/10.4103/1673-5374.390953
Date of submission: March 8, 2023
Date of decision: June 6, 2023
Date of acceptance: October 10, 2023
Date of web publication: December 15, 2023

## Graphical Abstract

*Biochanin A inhibits oxidative stress and inflammasome activation in a rat model of spinal cord injury*

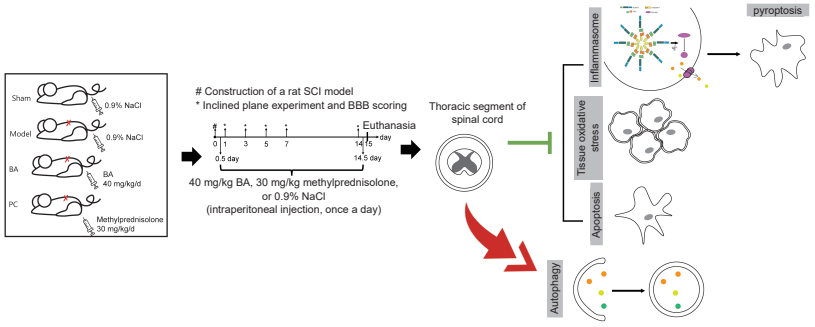


## From the Contents



## Abstract

Previous studies have shown that Biochanin A, a flavonoid compound with estrogenic effects, can serve as a neuroprotective agent in the context of cerebral ischemia/reperfusion injury; however, its effect on spinal cord injury is still unclear. In this study, a rat model of spinal cord injury was established using the heavy object impact method, and the rats were then treated with Biochanin A (40 mg/kg) via intraperitoneal injection for 14 consecutive days. The results showed that Biochanin A effectively alleviated spinal cord neuronal injury and spinal cord tissue injury, reduced inflammation and oxidative stress in spinal cord neurons, and reduced apoptosis and pyroptosis. In addition, Biochanin A inhibited the expression of inflammasome-related proteins (ASC, NLRP3, and GSDMD) and the Toll-like receptor 4/nuclear factor-κB pathway, activated the Nrf2/heme oxygenase 1 signaling pathway, and increased the expression of the autophagy markers LC3 II, Beclin-1, and P62. Moreover, the therapeutic effects of Biochanin A on early post-spinal cord injury were similar to those of methylprednisolone. These findings suggest that Biochanin A protected neurons in the injured spinal cord through the Toll-like receptor 4/nuclear factor κB and Nrf2/heme oxygenase 1 signaling pathways. These findings suggest that Biochanin A can alleviate post-spinal cord injury at an early stage.

**Key Words:** apoptosis; autophagy; Biochanin A; heme oxygenase 1; inflammation; Nrf2 protein; nuclear factor kappa-B; oxidative stress; spinal cord injury; Toll-like receptor 4

## Introduction

Spinal cord injury (SCI) can lead to irreversible motor and sensory dysfunction (Xue et al., 2020). The primary clinical symptom of SCI is motor dysfunction (Hurlbert et al., 2013). Moreover, histopathological analysis has shown that SCI induces hypoxia, neuronal apoptosis, and repair, as well as pathological changes such as congestion and necrosis in the spinal cord (Anjum et al., 2020). The pathological changes that occur after SCI are mainly divided into primary and secondary injuries (Gu et al., 2020). Mechanical injury is the main cause of primary injury, including falls from high places, sports injuries, and traffic accidents; histological and neurological injuries are the main secondary injuries, including ischemia, neuronal apoptosis, necrosis, edema, inflammatory response, and reactive oxygen species production (Ramer et al., 2014; Zhao et al., 2018). SCI morbidity and mortality primarily correlate with secondary injuries, so clinical treatment mainly focuses on this type of injury (Hewson et al., 2018; Garshick et al., 2019). Evidence suggests that inhibition of the NLR family pyrin domain-containing 3 (NLRP3) inflammasome can alleviate the damage caused by SCI (Jiang et al., 2017; Zhao et al., 2022). Furthermore, excessive oxidative stress is a key factor in SCI pathogenesis that can activate proinflammatory factors, the NLRP3 inflammasome, and pyroptosis in microglia (Liu et al., 2020; Khan et al., 2023; Chen et al., 2023). At present, SCI treatment mainly involves surgery, drugs, and rehabilitation (Liu et al., 2021a). Although these treatments can improve survival and quality of life in patients with SCI, they cannot restore damaged neurological function, and often have systemic side effects (Lu et al., 2020). Methylprednisolone has been shown to improve neurological outcomes in patients with acute SCI (Bracken, 2012), but it has systemic side effects, including cerebral hemorrhage, meningitis, conus syndrome, progressive weakness, reversible bladder dysfunction, and paresthesia (Canseco et al., 2021). Therefore, finding a safe, effective, and multi-target anti-SCI drug has become an important research priority.

In recent years, the use of monomer compounds derived from traditional Chinese medicines to treat SCI has gained much attention. Flavonoids are of particular interest (Zhang et al., 2018; Fan et al., 2019; Ma et al., 2023). For example, Yurtal et al. (2020) showed that hesperidin has anti-oxidative, anti-inflammatory, and anti-apoptotic neuroprotective and therapeutic effects in a rat model of SCI. Biochanin A (BA) is a methoxy isoflavone derived from leguminous plants such as chickpeas and *Trifolium pratense* L. that exhibits estrogen-like effects (Sarfraz et al., 2020).

Recent studies have shown that BA has various pharmacological effects, including anti-osteoporosis, anti-tumor, anti-oxidant, anti-inflammatory, and anti-apoptosis effects (Lee and Choi, 2005; Sarfraz et al., 2020; Guo et al., 2021). One study showed that BA mitigates cerebral ischemia/reperfusion damage by inhibiting apoptosis, endoplasmic reticulum stress, and the

[1]Department of Orthopedics, The First Affiliated Hospital of Zhejiang University, Hangzhou, Zhejiang Province, China; [2]Department of Stomatology, Xixi Hospital, Hangzhou, Zhejiang Province, China; [3]Department of Orthopedics, and Spine Surgery, the Affiliated Hospital of Xuzhou Medical School, the Second People's Hospital of Changshu, Changshu, Jiangsu Province, China
*Correspondence to: Xianfeng Lou, MD, Louxianfeng2022@yeah.net; Wenming Pan, MD, panwenming1982@sina.com.
https://orcid.org/0000-0003-3173-6929 (Xianfeng Lou); https://orcid.org/0009-0007-0866-8127 (Wenming Pan)
#Both authors contributed equally to this work.

***Funding:*** *This study was supported by the National Natural Science Foundation of China, Nos. LY20H090018 (to XL) and LY20H060008 (to HS).*
***How to cite this article:*** *Li X, Fu J, Guan M, Shi H, Pan W, Lou X (2024) Biochanin A attenuates spinal cord injury in rats during early stages by inhibiting oxidative stress and inflammasome activation. Neural Regen Res 19(9):2050-2056.*

mitogen-activated protein kinase 14 pathway, thus serving as an effective neuroprotectant (Guo et al., 2021). Another study showed that BA attenuates the acute lung injury caused by lipopolysaccharide by suppressing the toll-like receptor 4 (TLR4)/nuclear factor kappa-B (NF-κB) signaling pathway and up-regulating peroxisome proliferator activated receptor γ expression (Hu et al., 2020). However, whether BA has a protective effect in the context of SCI, and the mechanism underlying this potential effect, remain unclear.

The TLR4/NF-κB pathway is involved in NLRP3 inflammasome synthesis (Majidpoor et al., 2020). Evidence also suggests that activation of the nuclear factor erythroid-2 related factor 2 (Nrf2)/Heme oxygenase 1 (HO-1) signaling pathway can enhance neuronal cell resistance to oxidative stress, thereby protecting neural function (Lin et al., 2021; Xu et al., 2021). Therefore, the aim of this study was to investigate the potential therapeutic effect and of BA on early post-SCI, as well as the underlying mechanism, to provide a reference for SCI treatment .

## Methods

### Animals

Both male and female rats are commonly used in SCI models (Osimanjiang et al., 2022). Evidence suggests that males are more likely to develop SCI (Devivo, 2012), so male rats were used in this study. Forty adult (7-week-old) male Sprague-Dawley rats weighing 200 ± 20 g were obtained from Shanghai SLAC Laboratory Animal Co., Ltd. (Shanghai, China; SCXK (Hu) 2017-0005). The rats were raised in a specific pathogen-free laboratory animal barrier facility with a temperature- (22 ± 2°C) and humidity- (50–60%) controlled environment. All rats were acclimatized to 12 hours of light per day for 7 days, with food and water provided *ad libitum*. All experimental protocols were approved by the Experimental Animal Ethics Committee of Zhejiang Eyong Biotechnology Co., Ltd. (approval No. ZJEY-20211118-03) on November 18, 2021. The surgical procedures were carried out in accordance with the regulations of the China Animal Care and Use Committee.

### Construction of a rat model of spinal cord injury

Rats were randomly divided into four groups ($n$ = 10 rats per group): the sham, model, BA, and positive control (PC) groups. To induce SCI, the rats were deeply anesthetized with 2% pentobarbital sodium (Yuanye, Shanghai, China, R27405) by intraperitoneal injection at a dose of 30 mg/kg (Zhong et al., 2019). Next, the rats were placed in a prone position on a thermostat-controlled heating pad (37°C). A longitudinal incision was made along the midline of the rat's back to expose the paravertebral muscles, followed by further dissection to expose the T10 vertebra. Laminectomy was performed under an operating microscope to expose approximately 3 mm of the spinal dura. Then, SCI was induced via the standardized modified Allen's method (Hu et al., 2016), using a controlled impact device (RWD, Shenzhen, China, 68097) with a drop hammer weight of 8 g and a drop height of 40 mm to impact the spinal cord. Only laminectomy was performed in the sham group. Tetracycline (0.73 g/L, Yuanye, S17050) was added to the drinking water to prevent infection.

### Drug administration

Starting 12 hours after the surgery, rats in the BA and positive control groups were intraperitoneally injected with BA (Aladdin, Shanghai, China, Cat# B106472) at 40 mg/kg (Guo et al., 2019) and methylprednisolone (Sigma-Aldrich, Taufkirchen, Germany, Cat# BP248) at 30 mg/kg once a day. BA and methylprednisolone were dissolved in dimethyl sulfoxide (Yuanye, R21950) for storage and diluted with normal saline (0.9%, Yuanye, R27405) to their working concentrations: BA (40 mg/mL) and methylprednisolone (30 mg/mL). Rats in the sham and model groups were injected with equal volumes (1 mL/kg) of normal saline containing dimethyl sulfoxide intraperitoneally. Rats in all groups were continuously treated for 14 days. The experimental timeline is shown in **Additional Figure 1**.

### Inclined plane experiment

The inclined plane experiment was used to test the rats' ability to balance on elevated wooden beams. Hindlimb strength was assessed on the 1$^{st}$, 3$^{rd}$, 5$^{th}$, 7$^{th}$, and 14$^{th}$ days after surgery, according to the modified Rivlin's method (Rivlin and Tator, 1977). For this experiment, we constructed a movable plate with an adjustable angle (0–90°) using a smooth board (500 mm × 300 mm), a protractor, and a sturdy box as a support. The angle between the ramp and the horizontal plane was increased incrementally, and the maximum value of ramp angle at which each rat could maintain its posture for 5 seconds without falling was recorded.

### Basso-Beattie-Bresnahan scoring

Basso-Beattie-Bresnahan (BBB) scoring was used to assess the recovery of spinal cord function in each group of rats (Basso et al., 1995). On the 1$^{st}$, 3$^{rd}$, 5$^{th}$, 7$^{th}$ and 14$^{th}$ day after surgery, the motor function of the hindlimbs of the rats in each group was evaluated, and a BBB score was assigned. The BBB scores range from 0 to 21, where 0 means that the hindlimb has no motor ability, and 21 means that the hind limb has normal motor ability.

### Assessment of spinal cord edema

Spinal cord edema was assessed by measuring the wet/dry ratio of the spinal cord (Mao et al., 2011). After behavioral evaluation, rats were euthanized via $CO_2$ asphyxiation at a replacement rate of 40% by trained technicians. Rats were placed in a euthanasia chamber (Lab Animal Technology, Beijing, China, LAT-10-0090) filled with $CO_2$ until they stopped breathing and had lost all color in their eyes. Then, the fresh spinal cord tissue was collected and weighed to determine the wet weight. Next, the spinal cord tissue was dried in a 70°C incubator for 24 hours and weighed to determine the dry weight. The wet/dry weight ratio of the spinal cord was then calculated from the two values.

### Measurement of factors related to inflammation and oxidative stress

On the 15$^{th}$ day after injury, the spinal cords were harvested and homogenized using a high-throughput tissue grinder (E1644, Beyotime, Shanghai, China) at a frequency of 9.5 Hz for 20 minutes. The homogenized tissue was centrifuged (4°C, 5000 × $g$, 10 minutes), and the supernatant was collected. Interleukin 1β (IL-1β), interleukin 6 (IL-6), tumor necrosis factor-α (TNF-α), and interleukin 18 (IL-18) ELISA kits were purchased from MEIMIAN (Yancheng, Jiangsu, China). Superoxide dismutase (SOD), catalase (CAT), glutathione (GSH), and malondialdehyde (MDA) ELISA kits were obtained from Jiancheng (Nanjing, China). The content of these markers related to oxidative stress and inflammation in the spinal cords was determined by ELISA according to the kits manufacturers' instructions.

### Histological analysis

On days 15–20 after injury, spinal cords were harvested, fixed in 10% formalin (Leagene, Beijing, China, DF0110), dehydrated, and embedded in paraffin. The next day, the paraffin blocks were cut into 4-μm slices. The slices were subjected to xylol dewaxing, then rehydrated. Next, the slices were stained with hematoxylin (5 minutes), differentiated in 1% hydrochloric (30 seconds), counterstained with eosin (3 minutes), dehydrated, and permeablized with xylene. The hematoxylin and eosin (H&E) kit (BL700A) was purchased from Biosharp (Beijing, China). The slices were then mounted and sealed with neutral gum, and the tissue integrity was monitored under an optical microscope (Nikon, Tokyo, Japan, ECLIPSE 80i). The H&E scoring criteria used were described previously (Xiong et al., 2020). Briefly, the higher the score (range, 0–6) the more significant the inflammatory cell infiltration and tissue structure disorder. The slides were scored by two pathology experts who were blinded to the group assignments; spinal cord tissue from six rats in each group was assessed.

### Immunofluorescence staining

On the 21$^{st}$ day after surgery, immunofluorescence was performed to detect protein expression levels in spinal cord tissue. Tissue slices were generated as described in the Histological analysis subsection. In brief, after dewaxing and rehydrating the slices, antigen retrieval was performed by boiling 10-micrometer spinal cord slices in 10 mM sodium citrate buffer (pH 9.0, 80°C) for 0.5 hours. Each slice was blocked in 5% bovine serum albumin for 60 minutes at 37°C, then stained with Alexa Fluor® 488 anti-microtubule-associated protein light chain 3 (LC3) rabbit monoclonal antibody (1:50, CST, Danvers, MA, USA, Cat# 13082, RRID: AB_2687880), anti-SQSTM1/p62 rabbit polyclonal antibody (1:100, Affinity, Cincinnati, OH, USA Cat# AF5384, RRID: AB_2837869), and Alexa Fluor® 647 rabbit monoclonal anti-NeuN antibody (1:50, Abcam, Cambridge, UK, Cat# ab190565, RRID: AB_2732785) overnight at 4°C. 4,6-Diamino-2-phenylindole (DAPI; Beyotime, C1005) was used to stain the nuclei (37°C, 10 minutes, dark room). Stained slices from six rats each group were observed under a fluorescence microscope (Eclipse C1, Nikon), and Image Pro Plus 6.0 (Media Cybernetics, Rockville, MD, USA) was used to analyze the fluorescence intensity of the tissue slices.

### Terminal deoxynucleotidyl transferase mediated dUTP nick-end labeling assay

Spinal cord sections from six rats in each group were also assessed for apoptosis using terminal deoxynucleotidyl transferase (TdT) mediated dUTP nick-end labeling (TUNEL) staining (Servicebio, Wuhan, China, G1507) on the 21$^{st}$ day after surgery. Proteinase K was dripped onto the prepared slices (37°C, 30 minutes). Next, the slices were treated with 3% $H_2O_2$ at 37°C for 20 minutes. Next, the slices were washed, then treated with TdT incubation buffer followed by reaction with streptavidin-horseradish peroxidase (HRP) working solution. DAPI was used to stain the nuclei. After the slices were treated to make them transparent, they were blocked in neutral balsam. Afterwards, a fluorescence microscope was used to observe the positively staining cells. The apoptosis rate (%) was calculated as follows: number of positive cells/total number of cells × 100.

### Nissl staining

Paraffin-embedded spinal cord tissue harvested from six rats in each group on the 21$^{st}$ day after surgery was cut into 4-μm-thick slices. After dehydration and rehydration, the slices were soaked in Nissl stain solution (Solarbio, Beijing, China, G1436) at 60°C for 0.5 hours, then differentiated with 95% ethanol. After dehydration with anhydrous ethanol, clearing with xylene, and mounting with neutral gum, an optical microscope (ECLIPSE E100, Nikon, Tokyo, Japan) was used to count the number of Nissl bodies.

### Immunohistochemistry

Spinal cord slices (4-μm-thick) from six rats in each group were generated on the 22$^{nd}$ day after surgery, as described in the Histological analysis subsection. The sections were treated with 3% $H_2O_2$ solution in the dark for 25 minutes to block endogenous peroxidase. After rinsing in phosphate-buffered saline, the sections were sealed with 5% bovine serum albumin (37°C, 30 minutes) followed by incubation with an anti-apoptosis-associated speck-like protein containing CARD (ASC) rabbit polyclonal antibody (1:200, Affinity, Cat# DF6304, RRID: AB_2838270), anti-caspase-1 rabbit polyclonal antibody (1:200, Affinity, Cat# AF5418, RRID: AB_2837902), anti-NLRP3 rabbit polyclonal antibody (1:200, Affinity, Cat# DF7438, RRID: AB_2839376), and anti-Nrf2 rabbit polyclonal antibody (1:200, Affinity, Cat# AF0639, RRID: AB_2833793)

overnight at 4°C. Afterwards, goat anti-rabbit IgG (H+L) HRP (1:200, Affinity, Cat# S0001, RRID: AB_2839429) was added (37°C, 1 hour), the nuclei were counterstained with DAPI, and the slices were dehydrated and mounted with neutral balsam. An optical microscope was used to visualize the tissues, and Image Pro Plus 6.0 was used to determine the integrated optical density (IOD) and average density (AOD) = IOD/area. AOD was used to analyze immunopositivity.

**Quantitative reverse transcription–polymerase chain reaction (qRT-PCR)**
Except for the tissues used for staining, all other rat tissues were preserved at –80°C. qRT-PCR was performed on the 18th day after surgery. An RNA extraction kit (LS1040) purchased from Promega (Madison, WI, USA) was used to isolate RNA from the spinal cord tissue. The mRNA levels of NLRP3, ASC, Gasdermin D (GSDMD), and caspase-1 were detected using a qRT-PCR System (7500, ThermoFisher, Waltham, MA, USA) and a one-step qRT-PCR kit (A6020, Promega). The results were normalized to glyceraldehyde-3-phosphate dehydrogenase (GAPDH) and quantified using the $2^{-\Delta\Delta Ct}$ formula (Fan et al., 2020). The primers used in the qRT-PCR reaction are shown in **Table 1**.

**Table 1 | Primer sequence information for quantitative reverse transcription-polymerase chain reaction**

| Gene | Forward primer | Reverse primer | Product size (bp) |
|---|---|---|---|
| Rat NLRP3 | 5'-GAA CCT CGA GCT GAT CTT CG-3' | 5'-CTG AGC TCC GAT TCG AAG G-3' | 111 |
| Rat ASC | 5'-GCC CAC CAA CCC AAG CAA GAT G-3' | 5'-CTC CGC TCC AGG TCC TCC AC-3' | 112 |
| Rat GSDMD | 5'-GCC TCC ACA ACT TCC TGA CAG ATG-3' | 5'-GGT CTC CAC CTC TGC CCG TAG-3' | 115 |
| Rat caspase-1 | 5'-GAA CCT CGA GCT GAT CTT CG-3' | 5'-CTG AGC TCC GAT TCG AAG G-3' | 182 |
| Rat GAPDH | 5'-AAG GTC GGT GTG AAC GGA-3' | 5'-CTT TGT CAC AAG AGA AGG CAG C-3' | 70 |

**Western blot assay**
On the 18th day after surgery, three rats in each group were randomly selected for protein expression level detection. The spinal cords were harvested and homogenized in radioimmunoprecipitation assay buffer (20101ES60, Yeasen, Shanghai, China), and a bicinchoninic acid assay kit (P0011, Beyotime) was used to determined total protein content. Next, the proteins were separated on a 10% sodium dodecyl sulfate polyacrylamide gel and transferred to polyvinylidene fluoride membranes (FFP24, Beyotime), which were then blocked with 5% non-fat milk (37°C, 1 hour).

Thereafter, the membranes were exposed to diluted primary antibodies overnight at 4°C, followed by goat anti-rabbit IgG (H+L) HRP (1:10,000, Affinity, Cat# S0001, RRID: AB_2839429) or goat anti-mouse IgG (H+L) HRP (1:10,000, Affinity, Cat# S0002, RRID: AB_2839430) at 37°C for 60 minutes. The protein bands were detected with enhanced chemiluminescence reagent (GK10008, GlpBio, Montclair, CA, USA) and visualized on a gel imager (FluorChem FC3, Alpha, ProteinSimple, Silicon Valley, CA, USA). The primary antibodies used, which were purchased from Affinity, were as follows: anti-GSDMD rabbit polyclonal antibody (1:1000, Cat# AF4013, RRID: AB_2846780), anti-IL-18 rabbit polyclonal antibody (1:2000, Cat# DF6252, RRID: AB_2838218), anti-IL-1β rabbit polyclonal antibody (1:2000, Cat# AF5103, RRID: AB_2837589), anti-TLR4 rabbit polyclonal antibody (1:1000, Cat# AF7017, RRID: AB_2835322), anti-NF-κB P65 (P65) mouse monoclonal antibody (1:2000, Cat# BF8005, RRID: AB_2846809), anti-phospho-NF-κB P65 (p-P65) rabbit polyclonal antibody (1:2000, Cat# AF2006, RRID: AB_2834435), anti-phospho-NF-κB inhibitor alpha (IκBα) rabbit polyclonal antibody (1:1000, Cat# AF2002, RRID: AB_2834433), anti-IκBα rabbit polyclonal antibody (1:2000, Cat# AF5002, RRID: AB_2834792), anti-cleaved-caspase-3 rabbit polyclonal antibody (1:1000, Cat# AF7022, RRID: AB_2835326), anti-Bax rabbit polyclonal antibody (1:2000, Cat# AF0120, RRID: AB_2833304), anti-Bcl-2 rabbit polyclonal antibody (1:1000, Cat# AF6139, RRID: AB_10641852), anti-LC3I/II rabbit polyclonal antibody (1:500, Cat# AF5402, RRID: AB_2837886), anti-Beclin-1 rabbit polyclonal antibody (1:1000, Cat# AF5128, RRID: AB_2837614), anti-P62 rabbit polyclonal antibody (1:1000, Cat# AF5384, RRID: AB_2837869), anti-Nrf2 rabbit polyclonal antibody (1:2000, Cat# AF0639, RRID: AB_2833793), anti-HO-1 rabbit polyclonal antibody (1:2000, Cat# AF5393, RRID: AB_2837878), anti-GAPDH rabbit polyclonal antibody (1:20,000, Cat# AF7021, RRID: AB_2839421), and anti-β-actin rabbit polyclonal antibody (1:20,000, Cat# AF7018, RRID: AB_2839420). ImageJ (National Institutes of Health, Bethesda, MD, USA) (Schneider et al., 2012) was used to analyze the gray scale values of the bands, and all western blot data were normalized to the sham group.

**Statistical analysis**
Sample size was estimated using G.power 3.1 software (Heinrich-Heine-University Düsseldorf, Dusseldorf, Germany) (Faul et al., 2009) with $\alpha_{err\ prob} = 0.05$. A total of 40 rats were included in the experiment, and semi-quantitative analysis of all tissue staining was conducted using a blinded method. Quantitative tissue staining data from six independent experiments and quantitative qRT-PCR and Western blot data from three independent experiments are presented as mean ± standard deviation (SD). For statistical analyses, IBM SPSS software (Version 16.0., SPSS Inc., Chicago, IL, USA) was applied. One-way analysis of variance was used for comparisons among multiple groups, and pairwise comparisons between groups were performed using Tukey's *post hoc* test. $P < 0.05$ was considered statistically significant.

## Results

**Effects of BA on hindlimb recovery, edema, inflammatory factors, and oxidative stress in a rat model of spinal cord injury**
The inclined plane experiment and BBB scoring were used to assess recovery of spinal cord function. The angle of incline and BBB score were notably lower in the model group than in the sham group from the 1st day after surgery (all $P < 0.01$; **Figure 1A** and **B**). From the 5th day after surgery, BA alone and methylprednisolone alone significantly improved the angle of incline and BBB score in SCI rats (all $P < 0.01$; **Figure 1A** and **B**). In addition, the spinal cords had a higher wet/dry weight ratio in post-SCI rats than in sham rats ($P < 0.01$; **Figure 1C**), and BA alone and methylprednisolone alone dramatically improved the wet/dry weight ratio (both $P < 0.01$; **Figure 1C**). Next, to investigate the effect of BA and methylprednisolone on inflammation and oxidative stress in SCI rats, we performed ELISA analysis. Compared with sham rats, the SCI rats exhibited higher levels of inflammatory factor expression (IL-6, IL-1β, TNF-α, and IL-18) ($P < 0.01$; **Figure 1D–G**), higher oxidative stress levels ($P < 0.01$; **Figure 1H–J**), and lower antioxidant levels (CAT, SOD, and GSH) ($P < 0.01$; **Figure 1K**). The ELISA results showed that BA and methylprednisolone repressed inflammation and oxidative stress, as evidenced by decreased IL-6, IL-1β, TNF-α, IL-18, and MDA levels and increased CAT, SOD, and GSH levels in the spinal cord tissue of SCI rats ($P < 0.05$; **Figure 1D–K**). These findings indicate that BA improves hindlimb motor function and inhibits edema, inflammation, and oxidative stress in the spinal cords of SCI rats.

**BA ameliorates spinal cord damage at the histopathological level in a rat model of spinal cord injury**
H&E staining was performed to assessed damage at the histopathological levels in the spinal cords of SCI rats. Compared with the sham group, rats in the model group showed degeneration of spinal cord tissue neurons, damage to peripheral neurons, edema, degeneration of the myelin sheath in the white matter, and tissue structure disruption. BA and methylprednisolone improved all of these parameters (**Figure 2A**) and significantly reduced H&E staining scores in the spinal cord tissue of SCI rats compared with the findings in SCI rats ($P < 0.01$; **Figure 2B**). These findings indicate that BA ameliorates damage at the histopathological levels in the spinal rods of SCI rats.

**Effects of BA on apoptosis and the number of neurons in a rat model of spinal cord injury**
TUNEL staining and Nissl staining were performed to observe the degree of apoptosis and damage of neurons in spinal cord tissue, respectively. As shown in **Figure 3A** and **B**, the green fluorescence signal was strongest in the model group. The TUNEL staining results showed that the apoptosis rate in the spinal cord tissue was higher in the model group than in the sham group; more importantly, the apoptosis rate decreased after treatment with BA or methylprednisolone ($P < 0.01$). The Nissl staining results showed that most of the neurons in the spinal cord tissue of rats in the model group were in a pyknotic hyperchromatic state; whereas, in rats treated with BA and methylprednisolone, the number of neurons with intact cell structure increased, and the number of Nissl bodies was significantly increased ($P < 0.01$; **Figure 3C** and **D**). These results indicate that BA treatment inhibits apoptosis and increases the number of intact neurons in SCI rats.

**BA facilitates neuronal autophagy in the spinal cords of rats with spinal cord injury**
Next, immunofluorescence staining was used to measure LC3 and P62 expression in spinal cord tissue. Compared with that in the sham group, LC3 immunopositivity in the model group was significantly lower, while P62 immunopositivity was significantly higher ($P < 0.01$, **Figure 4A–D**). Interestingly, BA and methylprednisolone significantly increased LC3 immunopositivity and decreased P62 immunopositivity ($P < 0.01$, **Figure 4A–D**). These findings suggest that BA promotes neuronal autophagy in the spinal cord of SCI rats.

**BA regulates pyroptosis, inflammation, and antioxidation in a rat model of spinal cord injury**
We next used immunohistochemistry to observe the expression levels of markers related to the inflammasome (ASC and NLRP3), pyroptosis (caspase-1), and antioxidation (Nrf2) in spinal cord tissue. The results showed that ASC, caspase-1, and NLRP3 immunopositivity was significantly higher, while Nrf2 expression was significantly lower, in the model group than in the sham group (all $P < 0.01$, **Figure 5A–D**). Importantly, ASC, caspase-1, and NLRP3 levels were lower in SCI rats than in sham rats, while BA and methylprednisolone treatment increased Nrf2 expression (all $P < 0.01$, **Figure 5A–D**). Moreover, qRT-PCR analysis demonstrated that the expression of genes related to the inflammasome (ASC and NLRP3) and pyroptosis (caspase-1 and GSDMD) in spinal cord tissue was higher in SCI rats compared with that in the sham group and decreased in SCI rats treated with BA and methylprednisolone (all $P < 0.05$, **Figure 6A–D**). These findings suggest that BA may reduce neuroinflammation and improve antioxidation in the spinal cord of SCI rats. Western blot analysis confirmed that BA or methylprednisolone effectively decreased the expression levels of the inflammasome-related proteins NLRP3, ASC, and GSDMD (all $P < 0.05$, **Figure 6A–H**), the expression

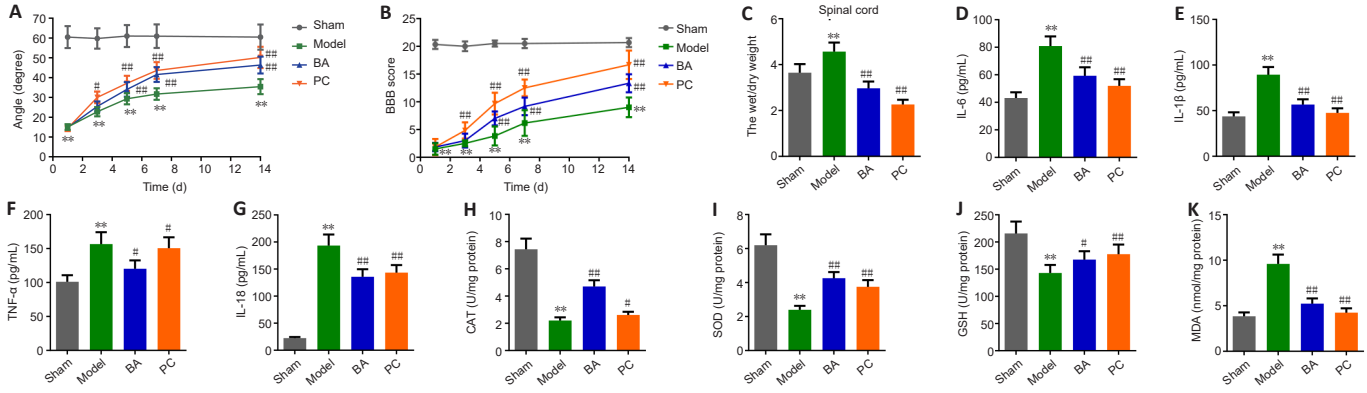


**Figure 1** | **The effect of BA on hindlimb recovery, edema, inflammatory factors, and oxidative stress in SCI rats.**
(A, B) On the 1st, 3rd, 5th, 7th, and 14th days after operation, BA-mediated promotion of hindlimb strength and motor function recovery in SCI rats was verified by inclined plane test (A) and BBB score (B), respectively. (C) On the 15th day, the wet/dry weight ratio of the spinal cord was used to evaluate the effect of BA on spinal cord edema. (D–K) Expression levels of the inflammatory factors IL-6 (D), IL-1β (E), TNF-α (F), and IL-18 (G) and the oxidative stress markers CAT (H), SOD (I), GSH (J), and MDA (K) in the spinal cord were determined by ELISA on the 15th day. Data are expressed as mean ± SD ($n$ = 6). $^{**}P < 0.01$, *vs.* sham group; $^{\#}P < 0.05$, $^{\#\#}P < 0.01$, *vs.* model group (one-way analysis of variance followed by Tukey's *post hoc* test). BA: Biochanin A; BBB: Basso Beattie Bresnahan; CAT: catalase; ELISA: enzyme-linked immunosorbent assay; GSH: glutathione; IL-18: interleukin-18; IL-1β: interleukin-1β; IL-6: interleukin-6; MDA: malondialdehyde; PC: positive control; SCI: spinal cord injury; SOD: superoxide dismutase; TNF-α: tumor necrosis factor-α.

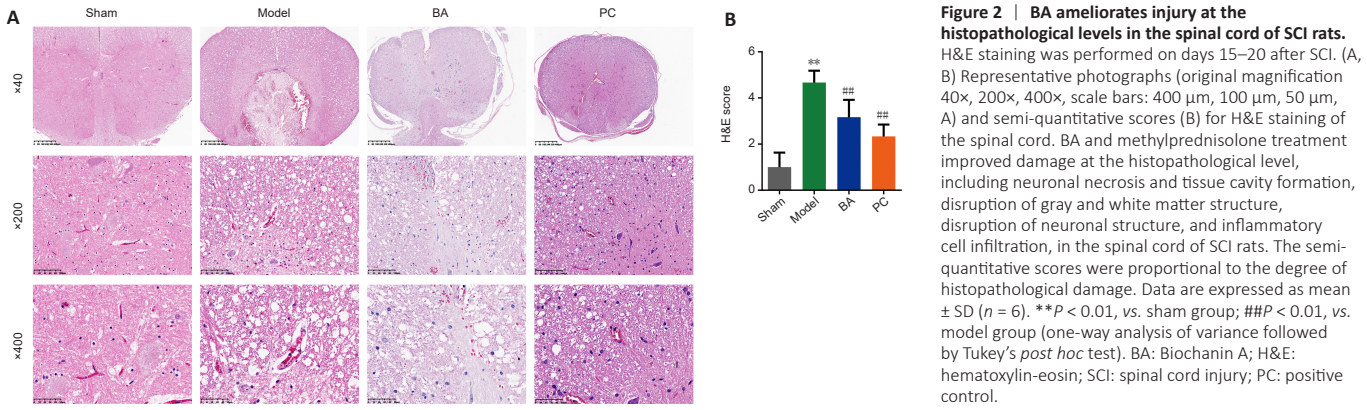


**Figure 2** | **BA ameliorates injury at the histopathological levels in the spinal cord of SCI rats.**
H&E staining was performed on days 15–20 after SCI. (A, B) Representative photographs (original magnification 40×, 200×, 400×, scale bars: 400 μm, 100 μm, 50 μm, A) and semi-quantitative scores (B) for H&E staining of the spinal cord. BA and methylprednisolone treatment improved damage at the histopathological level, including neuronal necrosis and tissue cavity formation, disruption of gray and white matter structure, disruption of neuronal structure, and inflammatory cell infiltration, in the spinal cord of SCI rats. The semi-quantitative scores were proportional to the degree of histopathological damage. Data are expressed as mean ± SD ($n$ = 6). $^{**}P < 0.01$, *vs.* sham group; $^{\#\#}P < 0.01$, *vs.* model group (one-way analysis of variance followed by Tukey's *post hoc* test). BA: Biochanin A; H&E: hematoxylin-eosin; SCI: spinal cord injury; PC: positive control.

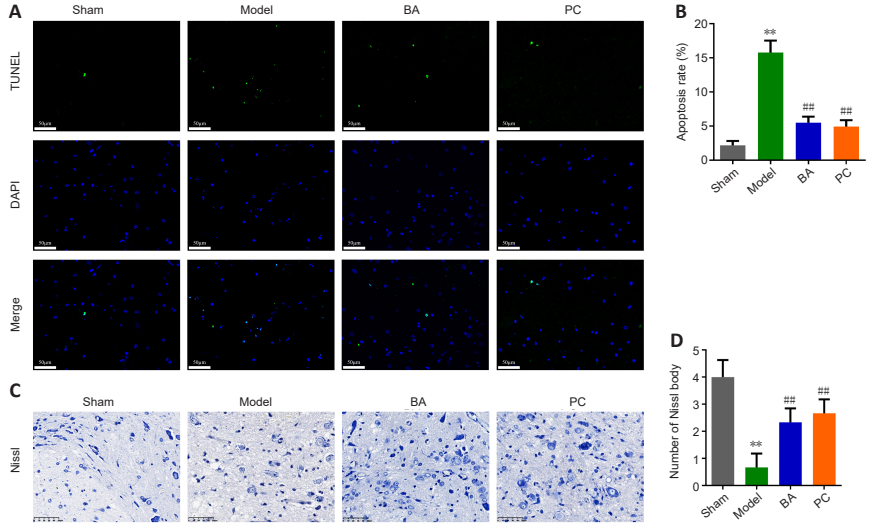


**Figure 3** | **On day 21 after injury, the effects of BA on neuronal apoptosis and neuron damage in SCI rats were observed.**
(A, B) The degree of apoptosis in the spinal cord of SCI rats was measured by TUNEL staining (original magnification 400×). The green fluorescence signal was strongest in the model group. BA and methylprednisolone treatment decreased the green fluorescence intensity. Scale bars: 50 μm. (C, D) The number of Nissl bodies in the anterior horn of the spinal cord in SCI rats was determined by Nissl staining (original magnification 400×). The model group exhibited fewer Nissl bodies than the sham group. BA and methylprednisolone treatment increased the number of Nissl bodies. Scale bars: 50 μm. Data are expressed as mean ± SD ($n$ = 6). $^{**}P < 0.01$, *vs.* sham group; $^{\#\#}P < 0.01$, *vs.* model group (one-way analysis of variance followed by Tukey's *post hoc* test). BA: Biochanin A; PC: positive control; SCI: spinal cord injury; TUNEL: terminal deoxynucleotidyl transferase dUTP nick end labeling.

levels of IL-18, IL-1β, and TLR4, and the ratios of p-P65/P65 and p-IκBα/IκBα in the spinal cord tissue of SCI rats compared with the findings in the model group (all $P < 0.05$, **Figure 6E**, **I–M**). These results show that BA suppresses pyroptosis, which may be related to the decreased inflammasome and increased antioxidation observed in the spinal cord of SCI rats.

**BA inhibits apoptosis and oxidative stress and promotes autophagy in a rat model of spinal cord injury**

Western blot analysis confirmed that BA and methylprednisolone prominently modulated the expression of markers of apoptosis (cleaved-caspase-3, Bax, and Bcl-2), autophagy (LC3II, LC3I, Beclin-1, and P62), and oxidative stress (Nrf2 and HO-1). Cleaved-caspase-3, Bax, and P62 were expressed at higher levels in SCI rats than in sham rats, while Bcl-2, LC3II/LC3I, Beclin-1, Nrf2, and HO-1 expression levels were lower (all $P < 0.01$, **Figure 7A–K**). Specifically, BA and methylprednisolone treatment decreased cleaved-caspase-3, Bax, and P62 protein levels and increased Bcl-2, LC3II/LC3I, Beclin-1, Nrf2, and HO-1 protein levels in the spinal cord tissue of SCI rats (all $P < 0.05$, **Figure 7A–K**). These results indicate that BA inhibits apoptosis and promotes autophagy and antioxidant stress in the spinal cord of SCI rats.

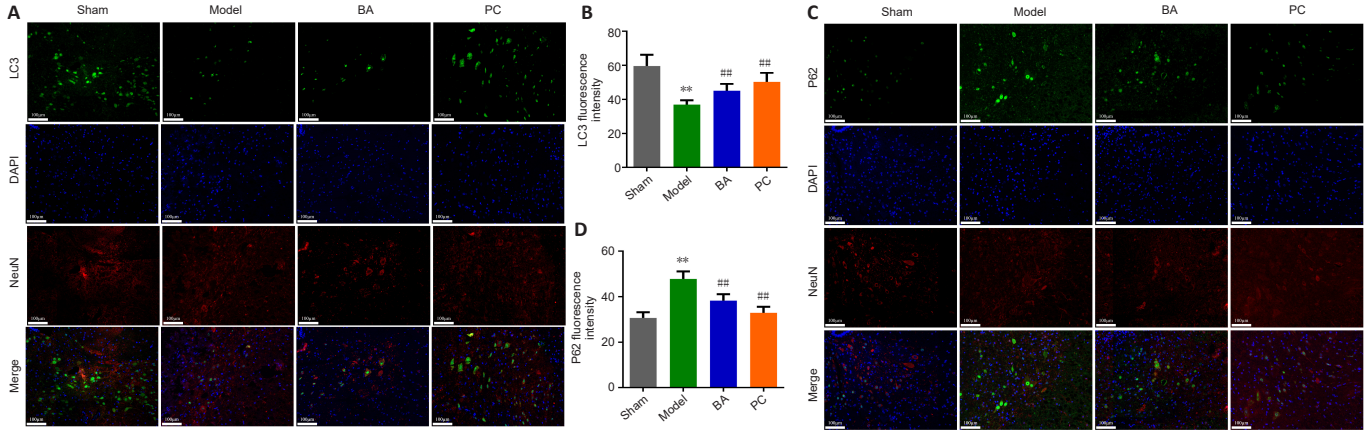


**Figure 4** | **On day 21 after injury, the promoting effect of BA on neuronal autophagy in the spinal cord tissue of SCI rats was observed.**
(A, B) Representative immunofluorescence images (A, original magnification 400×) and statistical analysis (B) of LC3 fluorescence intensity. LC3 fluorescence intensity (green Alexa Fluor® 488) was decreased in neurons (marked by NeuN, red, Alexa Fluor® 647) in the model group compared with that in the sham group; BA and methylprednisolone treatment enhanced LC3 fluorescence intensity (green, Alexa Fluor® 488). Scale bars: 100 µm. (C, D) Representative immunofluorescence images (C, original magnification 400×) and statistical analysis of P62 fluorescence intensity (D). Scale bars: 100 µm. P62 fluorescence intensity (green, Alexa Fluor® 488) in neurons (marked by NeuN, red, Alexa Fluor® 647) was stronger in the model group than in the sham group; BA and methylprednisolone treatment decreased P62 fluorescence intensity (green Alexa Fluor® 488). Data are expressed as mean ± SD ($n$ = 6). $^{**}P < 0.01$, *vs.* sham group; $^{\#\#}P < 0.01$, *vs.* model group (one-way analysis of variance followed by Tukey's *post hoc* test). BA: Biochanin A; DAPI: 4,6-diamino-2-phenylindole; LC3: microtube-associated protein 1 light-chain 3; P62: sequestosome-1; PC: positive control; SCI: spinal cord injury.

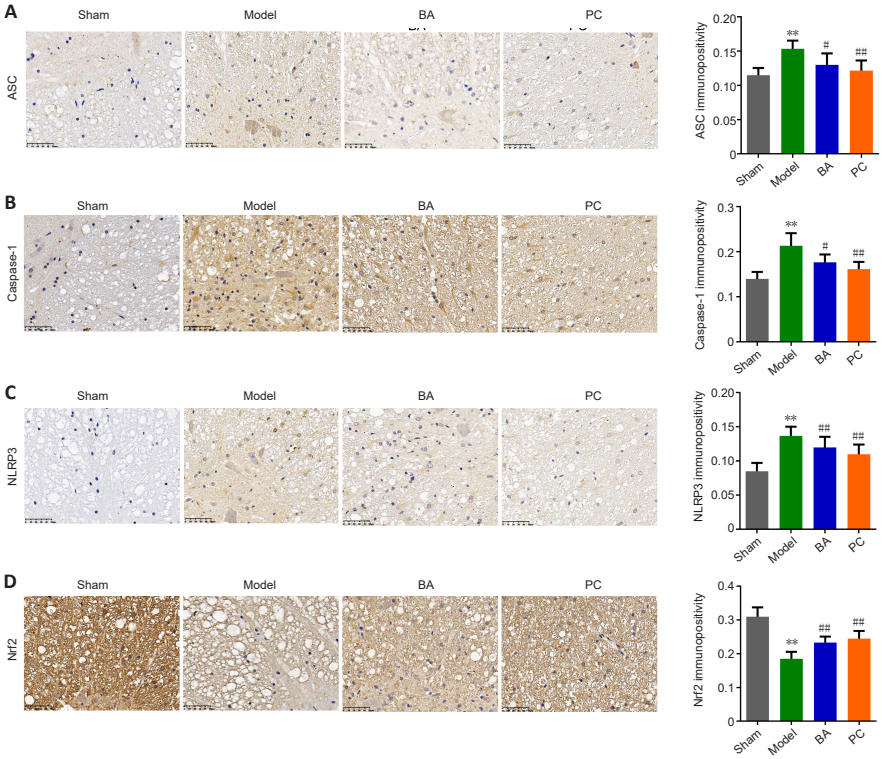


**Figure 5** | **BA suppresses pyroptosis and promotes anti-oxidation in the spinal cord of SCI rats.**
On day 22 after injury, immunohistochemistry was performed. (A–D) ASC (A), caspase-1 (B), NLRP3 (C), and Nrf2 (D) expression in the spinal cord was detected by immunohistochemistry (original magnification 400×). ASC, Caspase-1, and NLRP3 immunopositivity was higher in the model group than in the sham group, and BA and methylprednisolone treatment decreased the immunopositivity of all three proteins; while Nrf2 immunopositivity was decreased in model group and increased in rats treated with BA and methylprednisolone treatment. Scale bars: 50 µm. Data are expressed as mean ± SD ($n$ = 6). $^{**}P < 0.01$, *vs.* sham group; $^{\#}P < 0.05$, $^{\#\#}P < 0.01$, *vs.* model group (one-way analysis of variance followed by Tukey's *post hoc* test). AOD: Average optical density; ASC: apoptosis-associated speck-like protein containing CARD; BA: Biochanin A; NLRP3: NOD-like receptor thermal protein domain associated protein 3; Nrf2: nuclear factor erythroid2-related factor 2; PC: positive control; SCI: spinal cord injury.

## Discussion

In an *in vitro* study using PC12 cells treated with L-glutamate, Tan et al. (2013) found that BA played a neuroprotective role by impeding apoptosis. Our study confirms previous reports that BA exerts a neuroprotective effect by inhibiting apoptosis in the spinal cord, thus ameliorating SCI. In addition, numerous studies have shown that SCI is accompanied by oxidative stress injury (Pal et al., 2018; Torres-Espín et al., 2018). Nrf2 is a protective transcription factor that regulates oxidative stress responses in cells, and HO-1 is an antioxidant protease that can enhance the resistance of neuronal cells to oxidative stress and protect neural function (Lin et al., 2021; Xu et al., 2021). Abdel-Wahab et al. (2020) confirmed that the Nrf2/HO-1 signaling pathway is closely involved in oxidative stress-related diseases. Guo et al. (2019) demonstrated that BA protects the brain from ischemia/reperfusion injury by activating the Nrf2/HO-1 signaling pathway and suppressing the NF-κB pathway. In the current study we showed that BA suppresses oxidative stress in SCI rats, possibly through the Nrf2/HO-1 signaling pathway.

SCI is accompanied by inflammation. The TLR4 signaling pathway is one of the most significant inflammatory pathways; high TLR4 expression levels activate NF-κB, which in turn induces TLR4 activation by the cytokines TNF-α and IL-6, initiating a cascade reaction (Kang et al., 2015; Jia et al., 2019). We found that BA strongly repressed the TLR4 signaling pathway. In addition, NF-κB activation can further activate the caspase-3 pathway to mediate apoptosis (Xie et al., 2020). The expression levels of the apoptosis-related proteins cleaved-caspase-3 and Bax were significantly upregulated after SCI (Zhao et al., 2017). To further explore the effect of BA on SCI-induced apoptosis, we performed TUNEL, Nissl staining, and Western blotting. The results showed that BA inhibits spinal cord neuron apoptosis and has a neuroprotective effect on the central nervous system, which may be related to BA-mediated inhibition of the TLR4/NF-κB signaling pathway.

We also investigated changes in the expression of inflammasome-related genes and proteins in SCI rats treated with BA. A previous study suggested that activation of the NLRP3 inflammasome is a significant factor in secondary SCI injury and is involved in the maturation and release of NF-κB-related inflammatory factors (Liu et al., 2020). In addition, most neurological diseases involve pyroptosis (a form of programmed cell death) mediated by the NLRP3 inflammasome, and excessive pyroptosis can exacerbate the damage caused by SCI (Liu et al., 2021b).

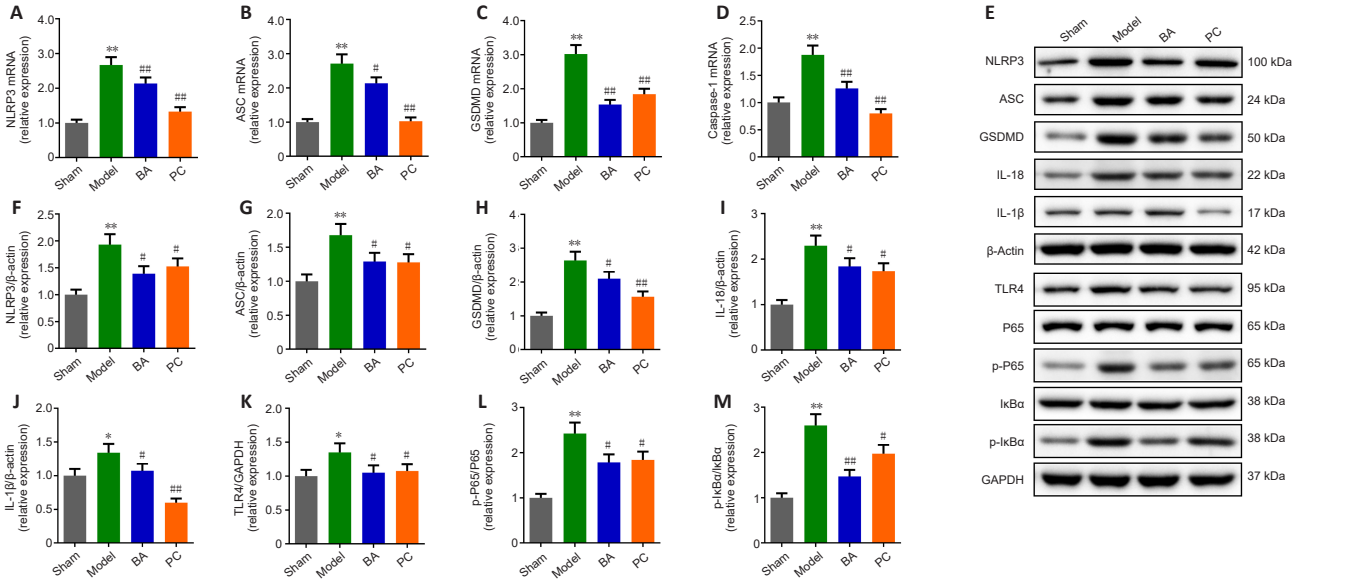


**Figure 6** | **BA alleviates pyroptosis and inflammation in the spinal cord tissue of SCI rats.**
On day 18 after SCI, Western blot assay was performed. (A–D) NLRP3 (A), ASC (B), GSDMD (C), and Caspase-1 (D) mRNA expression levels were measured by quantitative reverse transcription-polymerase chain reaction. (E) Western blot analysis of inflammation- and pyroptosis-associated protein expression levels. β-Actin was used as an internal reference for NLRP3, ASC, GADMD, IL-18, and IL-1β. GAPDH was used as an internal reference for TLR4, P65, p-P65, IκBα, and p-IκBα. (F–M) NLRP3 (F), ASC (G), GSDMD (H), IL-18 (I), IL-1β (J), TLR4 (K), p-P65/P65 (L), and p-IκBα/IκBα (M) protein expression levels were measured by Western blot assay. All western blot data were normalized to the sham group. Data are expressed as mean ± SD ($n$ = 3). *$P$ < 0.05, **$P$ < 0.01, *vs.* sham group; #$P$ < 0.05, ##$P$ < 0.01, *vs.* model group (one-way analysis of variance followed by Tukey's *post hoc* test). ASC: Apoptosis-associated speck-like protein containing CARD; BA: Biochanin A; GAPDH: glyceraldehyde-3-phosphate dehydrogenase; GSDMD: gasdermin D; IL-18: interleukin-18; IL-1β: interleukin-1β; NLRP3: NOD-like receptor thermal protein domain associated protein 3; PC: positive control; p-P65: phospho-NF-κB P65; p-IκBα: phospho-NF-kappa-B inhibitor alpha; SCI: spinal cord injury; TLR4: Toll-like receptor 4.

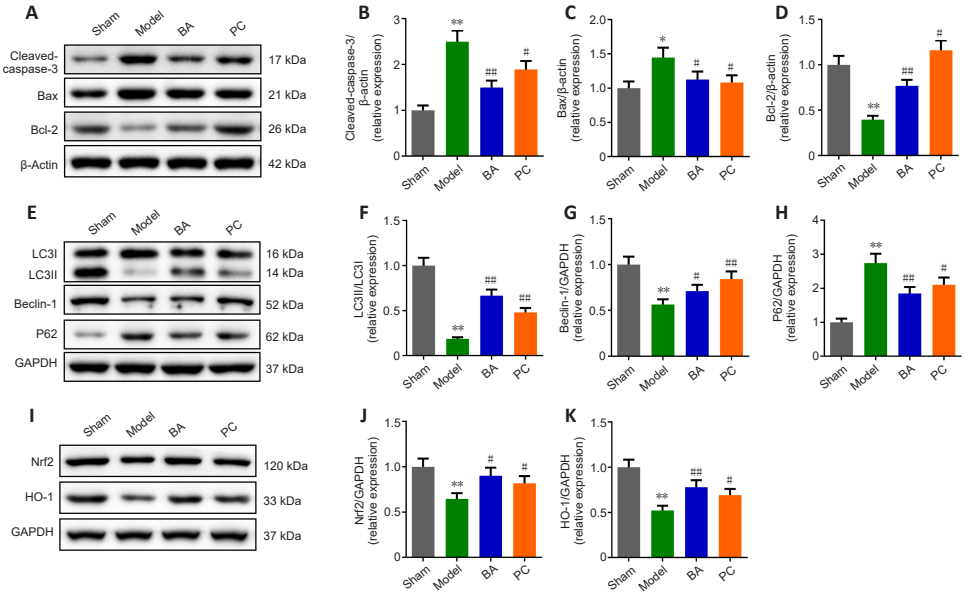


**Figure 7** | **BA inhibits apoptosis and oxidative stress and promotes autophagy in the spinal cord tissue of SCI rats.**
(A) Western blot analysis of apoptosis-related protein expression levels. (B–D) Quantification of cleaved-caspase-3 (B), Bax (C), and Bcl-2 (D) protein levels from the western blot data. (E) Western blot analysis of autophagy-related protein expression levels. (F–H) Quantification of LC3II/LC3I (F), Beclin-1 (G), and P62 (H) protein levels from the western blot data. (I) Western blot analysis of oxidative stress-related protein expression levels. β-Actin was used as an internal reference for cleaved-caspase-3, Bax, and Bcl-2. GAPDH was used as an internal reference for LC3I, LC3II, Beclin-1, P62, Nrf2, and HO-1. (J, K) Western blot analysis of Nrf2 (J) and HO-1 (K) protein expression levels. All western blot data were normalized to the sham group. Data are expressed as mean ± SD ($n$ = 3). **$P$ < 0.01, *vs.* sham group; #$P$ < 0.05, ##$P$ < 0.01, *vs.* model group (one-way analysis of variance followed by Tukey's *post hoc* test). BA: Biochanin A; HO-1: heme oxygenase-1; LC3: microtube-associated protein 1 light-chain 3; Nrf2: nuclear factor erythroid2-related factor 2; P62: sequestosome-1; PC: positive control; SCI: spinal cord injury.

It is worth noting that BA has been shown to attenuate myocardial ischemia/reperfusion injury by inhibiting activation of the TLR4/NF-κB/NLRP3 signaling pathway (Bai et al., 2019). Another study reported that BA alleviates renal interstitial fibrosis and inflammation by repressing the NF-κB/NLRP3 pathway (Ram et al., 2022). In the current study, we found that the NLRP3 inflammasome signaling pathway was suppressed. These findings suggest that BA may inhibit the NLRP3 inflammasome.

Autophagy-mediated modulation of the inflammasome has many complex functions (Harris et al., 2017). When the inflammasome is activated, autophagy can reduce pro-caspase-1 degradation and IL-1β release (Biasizzo and Kopitar-Jerala, 2020). A modulatory effect of BA treatment on the endophilin A2-FoxO3a-autophagy signaling pathway has been reported in a mouse model of angiotensin II-induced dopaminergic neuron injury (Yu et al., 2021). In the current study, we found that autophagy was inhibited in the spinal cord tissue of rats after SCI, while BA treatment activated autophagy. We demonstrated that BA alleviates SCI by reducing TLR4/NF-κB/NLRP3 signaling-induced inflammation and pyroptosis, which may relate to activation of autophagy.

The main limitation of this study is that we only demonstrated that BA can improve SCI and observed changes in apoptosis, autophagy, inflammasome, and pyroptosis levels. It remains unclear whether BA directly acts on the abovementioned pathways, and this should be explored further in follow-up studies. In addition, we mainly explored the role of BA in early post-SCI injury, but there is a lack of research on BA intervention at different time points post-SCI; thus, additional time points should be investigated. In addition, we did not address the complications and side effects of BA in our SCI model.

In conclusion, BA can improve motor dysfunction, reduce oxidative stress injury, the inflammatory response, and neuronal apoptosis, and promote autophagy in SCI rats, possibly through inhibition of the TLR4/NF-κB/NLRP3 signaling pathway and activation of the Nrf2/P62 signaling pathway.

**Author contributions:** *XL conceived and designed the study, and collected the data. MG was responsible for data analysis and interpretation and statistical analysis. JF wrote the manuscript. WP provided critical revision of the manuscript for intellectual content. XL and HS were responsible for funding raising. All authors read and approved the final version of the manuscript.*

**Conflicts of interest:** *All authors declare no conflicts of interest.*
**Data availability statement:** *All data generated or analyzed during this study are included in this published article and its Additional files.*

**Open peer reviewer:** *Aravin Kumar, National Neuroscience Institute, Singapore.*
**Additional files:**
***Additional Figure 1:*** *The timeline of SCI model construction and administration.*
***Additional file:*** *Open peer review report 1.*

## References

Abdel-Wahab BA, Alkahtani SA, Elagab EAM (2020) Tadalafil alleviates cisplatin-induced reproductive toxicity through the activation of the Nrf2/HO-1 pathway and the inhibition of oxidative stress and apoptosis in male rats. Reprod Toxicol 96:165-174.
Anjum A, Yazid MD, Fauzi Daud M, Idris J, Ng AMH, Selvi Naicker A, Ismail OHR, Athi Kumar RK, Lokanathan Y (2020) Spinal cord injury: pathophysiology, multimolecular interactions, and underlying recovery mechanisms. Int J Mol Sci 21:7533.
Bai Y, Li Z, Liu W, Gao D, Liu M, Zhang P (2019) Biochanin A attenuates myocardial ischemia/reperfusion injury through the TLR4/NF-κB/NLRP3 signaling pathway. Acta Cir Bras 34:e201901104.
Basso DM, Beattie MS, Bresnahan JC (1995) A sensitive and reliable locomotor rating scale for open field testing in rats. J Neurotrauma 12:1-21.
Biasizzo M, Kopitar-Jerala N (2020) Interplay between NLRP3 inflammasome and autophagy. Front Immunol 11:591803.
Bracken MB (2012) Steroids for acute spinal cord injury. Cochrane Database Syst Rev 1:CD001046.
Canseco JA, Karamian BA, Bowles DR, Markowitz MP, DiMaria SL, Semenza NC, Leibensperger MR, Smith ML, Vaccaro AR (2021) Updated review: The steroid controversy for management of spinal cord injury. World Neurosurg 150:1-8.
Chen GL, Sun K, Liu XZ, Tong KL, Chen ZJ, Yu L, Chen NN, Liu SY (2023) Inhibiting tau protein improves the recovery of spinal cord injury in rats by alleviating neuroinflammation and oxidative stress. Neural Regen Res 18:1834-1840.
Devivo MJ (2012) Epidemiology of traumatic spinal cord injury: trends and future implications. Spinal Cord 50:365-372.
Fan H, Tang HB, Shan LQ, Liu SC, Huang DG, Chen X, Chen Z, Yang M, Yin XH, Yang H, Hao DJ (2019) Quercetin prevents necroptosis of oligodendrocytes by inhibiting macrophages/microglia polarization to M1 phenotype after spinal cord injury in rats. J Neuroinflammation 16:206.
Fan H, Tang HB, Chen Z, Wang HQ, Zhang L, Jiang Y, Li T, Yang CF, Wang XY, Li X, Wu SX, Zhang GL (2020) Inhibiting HMGB1-RAGE axis prevents pro-inflammatory macrophages/microglia polarization and affords neuroprotection after spinal cord injury. J Neuroinflammation 17:295.
Faul F, Erdfelder E, Buchner A, Lang AG (2009) Statistical power analyses using G*Power 3.1: tests for correlation and regression analyses. Behav Res Methods 41:1149-1160.
Garshick E, Walia P, Goldstein RL, Teylan MA, Lazzari AA, Tun CG, Hart JE (2019) Associations between vitamin D and pulmonary function in chronic spinal cord injury. J Spinal Cord Med 42:171-177.
Gu J, Jin ZS, Wang CM, Yan XF, Mao YQ, Chen S (2020) Bone marrow mesenchymal stem cell-derived exosomes improves spinal cord function after injury in rats by activating autophagy. Drug Des Devel Ther 14:1621-1631.
Guo M, Lu H, Qin J, Qu S, Wang W, Guo Y, Liao W, Song M, Chen J, Wang Y (2019) Biochanin A provides neuroprotection against cerebral ischemia/reperfusion injury by Nrf2-mediated inhibition of oxidative stress and inflammation signaling pathway in rats. Med Sci Monit 25:8975-8983.
Guo MM, Qu SB, Lu HL, Wang WB, He ML, Su JL, Chen J, Wang Y (2021) Biochanin A alleviates cerebral ischemia/reperfusion injury by suppressing endoplasmic reticulum stress-induced apoptosis and p38MAPK signaling pathway in vivo and in vitro. Front Endocrinol (Lausanne) 12:646720.
Harris J, Lang T, Thomas JPW, Sukkar MB, Nabar NR, Kehrl JH (2017) Autophagy and inflammasomes. Mol Immunol 86:10-15.
Hewson DW, Bedforth NM, Hardman JG (2018) Spinal cord injury arising in anaesthesia practice. Anaesthesia 73 Suppl 1:43-50.
Hu J, Yang Z, Li X, Lu H (2016) C-C motif chemokine ligand 20 regulates neuroinflammation following spinal cord injury via Th17 cell recruitment. J Neuroinflammation 13:162.
Hu X, Qin H, Li Y, Li J, Fu L, Li M, Jiang C, Yun J, Liu Z, Feng Y, Yao Y, Yin B (2020) Biochanin A protect against lipopolysaccharide-induced acute lung injury in mice by regulating TLR4/NF-κB and PPAR-γ pathway. Microb Pathog 138:103846.
Hurlbert RJ, Hadley MN, Walters BC, Aarabi B, Dhall SS, Gelb DE, Rozzelle CJ, Ryken TC, Theodore N (2013) Pharmacological therapy for acute spinal cord injury. Neurosurgery 72 Suppl 2:93-105.
Jia H, Ma H, Li Z, Chen F, Fang B, Cao X, Chang Y, Qiang Z (2019) Downregulation of LncRNA TUG1 Inhibited TLR4 signaling pathway-mediated inflammatory damage after spinal cord ischemia reperfusion in rats via suppressing TRIL expression. J Neuropathol Exp Neurol 78:268-282.
Jiang W, Li M, He F, Zhou S, Zhu L (2017) Targeting the NLRP3 inflammasome to attenuate spinal cord injury in mice. J Neuroinflammation 14:207.
Kang N, Hai Y, Yang J, Liang F, Gao CJ (2015) Hyperbaric oxygen intervention reduces secondary spinal cord injury in rats via regulation of HMGB1/TLR4/NF-κB signaling pathway. Int J Clin Exp Pathol 8:1141-1153.
Khan M, Qiao F, Kumar P, Touhidul Islam SM, Singh AK, Won J, Singh I (2022) Neuroprotective effects of Alda-1 mitigate spinal cord injury in mice: involvement of Alda-1-induced ALDH2 activation-mediated suppression of reactive aldehyde mechanisms. Neural Regen Res 17:185-193.
Lee KH, Choi EM (2005) Biochanin A stimulates osteoblastic differentiation and inhibits hydrogen peroxide-induced production of inflammatory mediators in MC3T3-E1 cells. Biol Pharm Bull 28:1948-1953.
Lin W, Chen W, Liu K, Ma P, Qiu P, Zheng C, Zhang X, Tan P, Xi X, He X (2021) Mitigation of microglia-mediated acute neuroinflammation and tissue damage by heme oxygenase 1 in a rat spinal cord injury model. Neuroscience 457:27-40.
Liu H, Zhang J, Xu X, Lu S, Yang D, Xie C, Jia M, Zhang W, Jin L, Wang X, Shen X, Li F, Wang W, Bao X, Li S, Zhu M, Wang W, Wang Y, Huang Z, Teng H (2021a) SARM1 promotes neuroinflammation and inhibits neural regeneration after spinal cord injury through NF-κB signaling. Theranostics 11:4187-4206.
Liu Z, Yao X, Jiang W, Li W, Zhu S, Liao C, Zou L, Ding R, Chen J (2020) Advanced oxidation protein products induce microglia-mediated neuroinflammation via MAPKs-NF-κB signaling pathway and pyroptosis after secondary spinal cord injury. J Neuroinflammation 17:90.
Liu Z, Yao X, Sun B, Jiang W, Liao C, Dai X, Chen Y, Chen J, Ding R (2021b) Pretreatment with kaempferol attenuates microglia-mediate neuroinflammation by inhibiting MAPKs-NF-κB signaling pathway and pyroptosis after secondary spinal cord injury. Free Radic Biol Med 168:142-154.
Lu Y, Yang J, Wang X, Ma Z, Li S, Liu Z, Fan X (2020) Research progress in use of traditional Chinese medicine for treatment of spinal cord injury. Biomed Pharmacother 127:110136.
Ma RX, Liu P, Zhang Q, Zeng GF, Zong SH (2023) Molecular mechanism of total flavonoids of hawthorn leaves regulating astrocytes to repair spinal cord injury. Zhongguo Zuzhi Gongcheng Yanjiu 27:5327-5333.
Majidpoor J, Khezri Z, Rostamzadeh P, Mortezaee K, Rezaie MJ, Fathi F, Abouzaripour M, Bariki MG, Moradi F, Shirazi R, Joghataei MT (2020) The expressions of NLRP1, NLRP3, and AIM2 inflammasome complexes in the contusive spinal cord injury rat model and their responses to hormonal therapy. Cell Tissue Res 381:397-410.
Mao L, Wang HD, Pan H, Qiao L (2011) Sulphoraphane enhances aquaporin-4 expression and decreases spinal cord oedema following spinal cord injury. Brain Inj 25:300-306.
Osimanjiang W, Allgood JE, Van Sandt RL, Burns DT, Bushman JS (2022) Sexual dimorphism in lesion size and sensorimotor responses following spinal cord injury. Front Neurol 13:925797.
Pal A, Kumar S, Jain S, Nag TC, Mathur R (2018) Neuroregenerative effects of electromagnetic field and magnetic nanoparticles on spinal cord injury in rats. J Nanosci Nanotechnol 18:6756-6764.
Ram C, Gairola S, Syed AM, Kulhari U, Kundu S, Mugale MN, Murty US, Sahu BD (2022) Biochanin A alleviates unilateral ureteral obstruction-induced renal interstitial fibrosis and inflammation by inhibiting the TGF-β1/Smad2/3 and NF-kB/NLRP3 signaling axis in mice. Life Sci 298:120527.
Ramer LM, Ramer MS, Bradbury EJ (2014) Restoring function after spinal cord injury: towards clinical translation of experimental strategies. Lancet Neurol 13:1241-1256.
Rivlin AS, Tator CH (1977) Objective clinical assessment of motor function after experimental spinal cord injury in the rat. J Neurosurg 47:577-581.
Sarfraz A, Javeed M, Shah MA, Hussain G, Shafiq N, Sarfraz I, Riaz A, Sadiqa A, Zara R, Zafar S, Kanwal L, Sarker SD, Rasul A (2020) Biochanin A: A novel bioactive multifunctional compound from nature. Sci Total Environ 722:137907.
Schneider CA, Rasband WS, Eliceiri KW (2012) NIH Image to ImageJ: 25 years of image analysis. Nat Methods 9:671-675.
Tan JW, Tham CL, Israf DA, Lee SH, Kim MK (2013) Neuroprotective effects of biochanin A against glutamate-induced cytotoxicity in PC12 cells via apoptosis inhibition. Neurochem Res 38:512-518.
Torres-Espín A, Forero J, Fenrich KK, Lucas-Osma AM, Krajacic A, Schmidt E, Vavrek R, Raposo P, Bennett DJ, Popovich PG, Fouad K (2018) Eliciting inflammation enables successful rehabilitative training in chronic spinal cord injury. Brain 141:1946-1962.
Xie XK, Xu ZK, Xu K, Xiao YX (2020) DUSP19 mediates spinal cord injury-induced apoptosis and inflammation in mouse primary microglia cells via the NF-kB signaling pathway. Neurol Res 42:31-38.
Xiong Y, Xia Y, Deng J, Yan X, Ke J, Zhan J, Zhang Z, Wang Y (2020) Direct peritoneal resuscitation with pyruvate protects the spinal cord and induces autophagy via regulating PHD2 in a rat model of spinal cord ischemia-reperfusion injury. Oxid Med Cell Longev 2020:4909103.
Xu Y, Lu X, Zhang L, Wang L, Zhang G, Yao J, Sun C (2021) Icaritin activates Nrf2/Keap1 signaling to protect neuronal cells from oxidative stress. Chem Biol Drug Des 97:111-120.
Xue W, Tan W, Dong L, Tang Q, Yang F, Shi X, Jiang D, Qian Y (2020) TNFAIP8 influences the motor function in mice after spinal cord injury (SCI) through meditating inflammation dependent on AKT. Biochem Biophys Res Commun 528:234-241.
Yu YG, Han JH, Xue HX, Li WZ, Wu WN, Yin YY (2021) The variations of endophilin A2-FoxO3a-autophagy signal in angiotensin II-induced dopaminergic neuron injury mouse model and by biochanin A. Can J Physiol Pharmacol 99:1298-1307.
Yurtal Z, Altug ME, Unsaldi E, Secinti IE, Kucukgul A (2020) Investigation of neuroprotective and therapeutic effects of hesperidin in experimental spinal cord injury. Turk Neurosurg 30:899-906.
Zhang Q, Zhang LX, An J, Yan L, Liu CC, Zhao JJ, Yang H (2018) Huangqin flavonoid extraction for spinal cord injury in a rat model. Neural Regen Res 13:2200-2208.
Zhao H, Chen S, Gao K, Zhou Z, Wang C, Shen Z, Guo Y, Li Z, Wan Z, Liu C, Mei X (2017) Resveratrol protects against spinal cord injury by activating autophagy and inhibiting apoptosis mediated by the SIRT1/AMPK signaling pathway. Neuroscience 348:241-251.
Zhao SJ, Zhou W, Chen J, Luo YJ, Yin GY (2018) Bioinformatics analysis of the molecular mechanisms underlying traumatic spinal cord injury. Mol Med Rep 17:8484-8492.
Zhao YJ, Qiao H, Liu DF, Li J, Li JX, Chang SE, Lu T, Li FT, Wang D, Li HP, He XJ, Wang F (2022) Lithium promotes recovery after spinal cord injury. Neural Regen Res 17:1324-1333.
Zhong ZX, Feng SS, Chen SZ, Chen ZM, Chen XW (2019) Inhibition of MSK1 promotes inflammation and apoptosis and inhibits functional recovery after spinal cord injury. J Mol Neurosci 68:191-203.

*C-Editor: Zhao M; S-Editors: Yu J, Li CH; L-Editors: Crow E, Song LP; T-Editor: Jia Y*

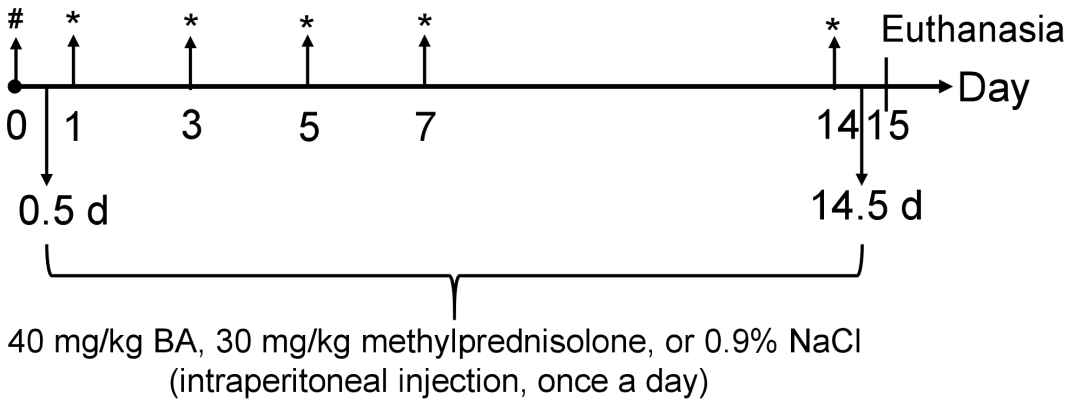


**Additional Figure 1 The timeline of SCI model construction and administration.**

# Construction of a rat SCI model; * inclined plane experiment and BBB scoring. BA: Biochanin A; NaCl: sodium chloride.

# OPEN PEER REVIEW REPORT 1

**Name of journal:** Neural Regeneration Research
**Manuscript NO:** NRR-D-23-00357
**Title:** Biochanin A attenuates spinal cord injury in rats by modulating Nrf2/P62 and TLR4/NF-κB/NLRP3 pathways
**Reviewer's Name:** Aravin Kumar
**Reviewer's country:** Singapore

## COMMENTS TO AUTHORS

This is a well written article with relevance to spinal cord injury and neuroprotection. The results are encouraging to the field of spinal cord injury management, even though these are still based on an animal model. My comments are below:

1. The authors should explicitly state the difference between the sham group and the model group. This would help to explain the differences in the results between the sham group, model group and the BA group, so as to make sense of the effectiveness of the intervention.
2. Is the BA infusion rate of 40mg/kg/d supported in the literature?
3. Were any perioperative complications observed in the mice especially in the BA group and PC group? This is of interest as we know that steroids result in wound complications in the human population with spinal cord injury, and this serves as one of the criticisms of its use. If the authors did not specifically look out for these complications, that should also be stated so that future studies can consider that during study design.
4. The timing for intervention is of particular interest in spinal cord injury - some groups advocate the administration of therapeutics such as steroids within 8H of spinal cord injury. Did the authors consider the time (in hours) after spinal cord injury for which BA or Methylprednisolone was administered - and was this controlled for?
5. The authors should include a paragraph on the limitations of the study.